ARCHITECTURE CIVIL ENGINEERING ENVIRONMENT
The Silesian University of Technology No. 1/2020

doi: 10.21307/ACEE-2020-007

SHAPING OF AXIALLY COMPRESSED BIPOLARLY PRESTRESSED CLOSELY SPACED BUILT-UP MEMBERS

Monika SIEDLECKA *

*PhD Eng.; Kielce University of Technology, Faculty of Civil Engineering and Architecture, Al. Tysiąclecia Państwa Polskiego 7, 25-314 Kielce, Poland
E-mail address: *monikach@tu.kielce.pl*

Received: 5.09.2019; Revised: 18.11.2019; Accepted: 28.12.2019

Abstract

The paper presents a method of shaping and describing the geometry of bipolarly prestressed closely spaced built-up member with symmetrical supports and a bisymmetrical cross-section. The following has been defined as a function dependant on the position along the length of the x section of the closely spaced built-up member with determined geometrical parameters: intial elastic $y_0(x)$ of the closely spaced built-up member chord in the prestressing zone, distance between the chords in the clear $s_i(x)$, moment of inertia $J_i(x)$ relative to main axes and eccentricity $e_i(x)$ of compressive force in a single chord. The length of the extreme section L_1 and the prestressing zone L_2, the maximum distance between chords s_{max} in the clear and the geometric characteristics of a single chord section were assumed. A full and correct description of the geometry of bipolarly prestressed closely spaced built-up members is necessary to start the static and stress analysis. As a result of the introduction of a bipolar displacement prestressing into the closely spaced built-up member, the moment of inertia increases in the middle part with respect to the non-material axis z. It allows predicting the increase of the critical load bearing capacity of the closely spaced built-up member. The load bearing capacity of bipolarly prestressed closely spaced built-up members was estimated using the modified Engesser's formula for two-chord closely spaced built-up member with rigid battens. For selected pair of channel sections, the analytical critical load estimation results were verified using FEM.

Keywords: **Axially compressed member; Bipolarly prestressed member; Bipolarly prestressed closely spaced built-up member; Bisymmetrical cross-section; Closely spaced built-up member; Load-bearing capacity.**

NOMENCLATURE

BPCSBUM	bipolarly prestressed closely spaced built-up member
CSBUM	closely spaced built-up member
$e_{z,ch}$	centre of gravity of the cross-section of one chord of the closely spaced built-up member to the z-axis;
f	maximum deflection;
$i_{ch,min}$	minimum inertia radius of one chord;
$i_{z,ch}$	radius of inertia with respect to the z-axis from one chord of the closely spaced built-up member;
$s_i(x)$	distance in the clear between the chords;
s_{max}	maximum distance in the clear between the chords in the middle of the member span, equivalent to the spacer thickness;
t_d	spacer thickness;
A_{ch}	cross-sectional area of one chord of the closely spaced built-up member;
E	Young's modulus;
$J_{y,ch}$	moment of inertia relative to the y axis of one chord of the closely spaced built-up member;
J_{z1}, J_{z2}, J_{z3}	moment of inertia of a composite section;
$J_{z,sr}$	equivalent moment of inertia to the z-axis;

L	total member length;
L_1	extreme section length with straight member;
L_2	prestressing zone length; prestressing range;
L_b	distance between friction grip bolts;
L_s	distance from the member edge to the first of the bolts joining the chords;
N_{cr}^{Eng}	Engesser critical load capacity;
N_{cr}^{mod}	modified Engesser critical load capacity;
N_e	Euler critical buckling load;
N_{eb}	modified Euler critical buckling load;
S_v	shear stiffness;

1. INTRODUCTION

The closely spaced built-up members (CSBUM) are used in engineering structures, such as columns, bracings, chords or diagonal braces of flat and spatial structures, among others: girders, space structures, domes, masts, towers and high-voltage line support structures. They are in the form of at least two component members, called chords, joined together in the welding process or with mechanical fasteners, e.g. rivets, bolts, one-sided bolts: spacerless (Fig. 1 a, b, g, h), with spacers (Fig. 1 c, d, i, j) or battens (Fig. 1 e, f, k, l).

Among the most commonly used composite CSBUMs sections there are channel sections (Fig. 1a-f) and cross-sections of two angle sections (Fig. 1g-l).

Since the early 20th century, CSBUMs made of two angle sections or channel sections have been the standard cross-section of light trusses, welded trusses of medium load, riveted trusses and truss crane beams [1, 2, 3]. Similarly, in flat, single- and double-curved space structures built since the 1950 with pyramidal-lateral assembly systems, e.g. Space-Deck (1954) [4, 5] Pyramitec (1960) [4, 5, 6, 7], Zachód (1970) [5, 8, 9, 10, 11] or Mostostal (1979) [5], twin members of the compressed upper chord were obtained as a result of back-to-back joining of adjacent pyramids and/or flat frames.

There is an extensive literature on load bearing capacity and stability of the multiple-chord members, including CSBUMs. It should be noted that failure to consider or underestimate shearing force impact on the load bearing capacity of multiple-chord members have caused construction failures and disasters many times in history [12]. Starting from Engesser [13] and Harringx [14] through Bleich [15], Timoshenko and Gere [16], to contemporary Kowal [17] and Bažant [18], many researchers proposed different calculation models to determine the critical load bearing capacity of a compressed member sensitive to shearing. Aslani and Goel [19] showed that the assumption of Timoshenko and Gere [16] is correct for multiple-chord members with widely spaced chords, while for the CSBUMs, it is too conservative. The separation coefficient modified by Aslani and Goel [19] gave more accurate results of ratio of slenderness, with a

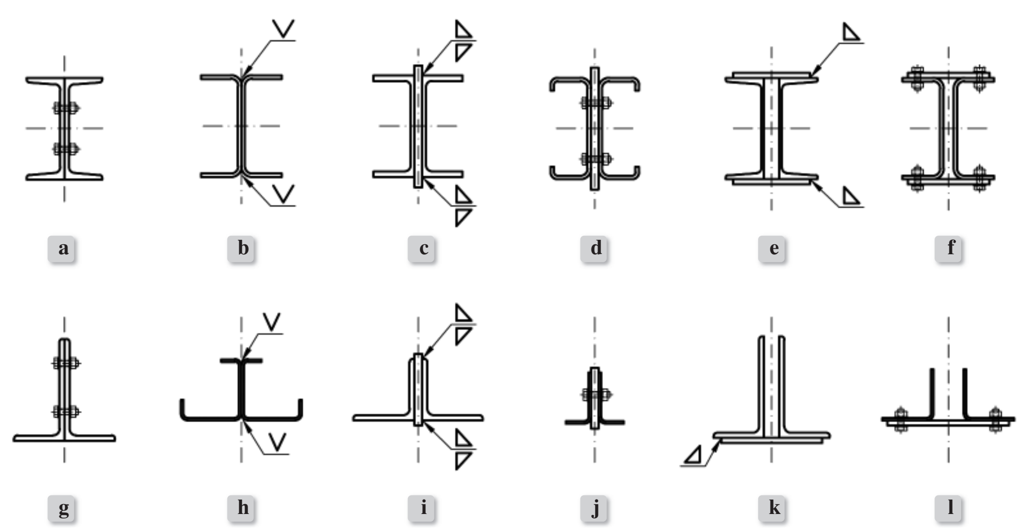

Figure 1.
Examples of composite closely spaced built-up member (CSBUM) sections built of a pair of: (a)–(f) channel sections, (g)–(l) angle sections

better approximation to Bleich [15] than in the approach of Timoshenko and Gere [16], and the proposed formula for the effective global ratio of slenderness of multiple-chord member with welded joints and/or fully-coupled connections has been introduced to later editions of the standard [20]. Temple and El-Mahdy [21, 22] proposed a conservative simplification of the formula for the ratio of slenderness of multiple-chord members with rigid battens and CSBUMs. Kowal [17] proposed the model of non-linear local interaction and global critical load bearing capacity, taking into account the amplification of local transverse displacement and derived an equation that solves the critical strength of a two-chord member joined by rigid battens.

Lue *et al.* [23] and Liu *et al.* [24] conducted experimental tests on CSBUMs made of rolled back-to-back channel sections with welded spacers, as well as bolted ones. The purpose of the experiment was to verify the standard formulas describing the ratio of slenderness of a multiple-chord member. Reference was made to Bleich's solution [15], and to standards [25–27]. Abejide and Masce [28] conducted a theoretical study on CSBUMs made of rolled back-to-back angles sections. The aim of the research was to estimate the length of effective members suitable for diagonal bracing, taking into account their safety and economy, as well as to conduct evaluation based on the standards [25, 29–31].

The interest in cross-sections of cold-formed members, especially thin-walled, has begun to grow since the end of the 20th century. Stone and La Boube [32] conducted experimental tests of back-to-back channel sections to verify provisions of the North American Specification for the Design of Cold-Formed Steel Structural Members. Ting and Lau [33] theoretically analyzed using the Effective Width Method and the Direct Strength Method and experimentally tested the compressed columns with two lipped channel placed back-to-back with batten cross-sections and joined by self-driving screw showing good agreement with results obtained. Anbarasu, Kanagarasu and Sukumar [34] supplemented the studies of Ting and Lau [33] with the FEM solution. Zhang and Young [35] presented the results of the experiment and the numerical FEM solution with non-linear analysis for compressed members with a cross-section of pair of spacerless sections Σ. Tamai *et al.* [36] theoretically analyzed and conducted experiments for members made of high-strength steel channel sections with spacers.

There are known methods of strengthening compressed members of metal structures by increasing the surface area and/or radius of inertia of the cross-section by joining (welding, gluing, mechanical joining) of additional components, such as sheets or sections to obtain a multiple-chord cross-section. Słowiński and Wuwer [37, 38] increased the cross-section of compressed CSBUM by tightening with one-sided BOM bolts of two channel sections to obtain a symmetrical three-chord member. Deniziak and Winkelmann [39, 40] analyzed a compressed member with a thin-walled channel section, doubled on a certain section and forming a monosymmetric CSBUM.

According to the standard [41], the compressed CSBUMs should be dimensioned in a similar way to uniform built-up compression members according to 6.4. Simplification of calculations and treatment of a composite member, spacerless or uniform with spacers, as a result of omitting shear stiffness ($S_v = \infty$), is recommended if the spacing between the centre of joints does not exceed $15 i_{ch,min}$ – where $i_{ch,min}$ is the minimum inertia radius of one chord. This condition applies to both, bolt fastenings and welded joints. The condition regarding spacing of connections, nota bene formulated decades ago for riveted connections, has not yet been verified. Because the spacing of connections usually exceeds $15 i_{ch,min}$, the topic was undertaken to shape CSBUMs with the use of fewer fasteners along the member and using bipolar prestressing with displacement [42].

The bipolar displacement prestressing presented in the paper is an innovative method. In the literature on the subject, axially compressed, built-up members, including CSBUMs, shaped in the proposed way, have not been found.

Because in the CSBUMs with compressive axial force it is possible to increase the critical load bearing capacity by introducing bipolar displacement prestressing [42], the correct description of the bipolarly prestressed closely spaced built-up member (BPCSBUM) geometry is necessary to conduct static and strength analyzes.

2. DEFINITION OF BPCSBUM

Bipolar prestressing is a controlled, permanent, symmetrical displacement of the CSBUM chord, relative to each other (Fig. 2), as a result of which self-balanced prestresses are introduced into the model. An innovative design of the BPCSBUM is obtained, characterized by a straight-line axis and non-linear course of the chord (Fig. 2c, 3). Bipolar prestressing

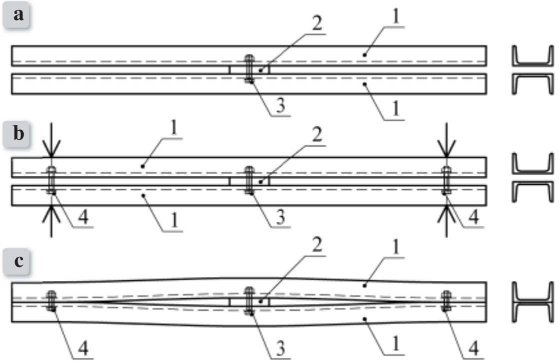

Figure 2.
Bipolar prestressing diagram of prestressed CSBUM with symmetrical boundary conditions [42]
(a) part A, (b) part B, (c) bipolarly prestressed closely spaced built-up member (BPCSBUM)
1 – chord of the CSBUM, 2 – spacer, 3 – spacer connector, 4 – friction grip bolt

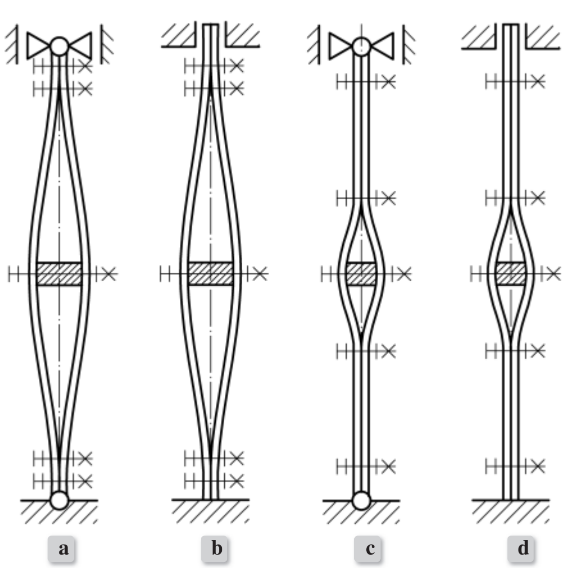

Figure 3.
Exemplary diagrams of BPCSBUMs

is introduced in CSBUMs with a cross-section where, as a result of flexural buckling, consistent with the first shape, the greatest displacement between joints would potentially occur.

Figure 2 presents a schematic diagram of the bipolar prestressing of a CSBUM of symmetric boundary conditions to the transverse axis. This process was divided into two A and B parts. In part A (Fig. 1a) a spacer was inserted in the form of a bolt-fastened plate in the middle of the member. In part B (Fig. 1b) the section, in which the spacer is present, is protected against translational and rotational displacements in all directions. And then, chords were joined with friction grip bolts in two cross-sections, located symmetrically to the centre of the member.

Figure 3 presents examples of BPCSBUM diagrams with different lengths of the prestressing zone and two-sided pinned or rigid support.

As a result of bipolar energy introduced into CSBUM with symmetrical support, a spindle-shaped BPCSBUM is obtained.

There are separated extreme straight lines, located symmetrically to the center, with the length L_1 and L_2 in the middle section, in the BPCSBUM, the chord course of which is non-linear. The division points into sections were associated with cross-sections with friction grip bolts. Thesection L_2, on which prestresses are introduced in the prestressed member, and the chord course is non-linear, is called the prestressing zone length or the prestressing range. The distance from the edge to the extreme bolt was marked as L_s. The spacer is provided in the form of plate of a fixed thickness t_d with a hole in a middle of it.

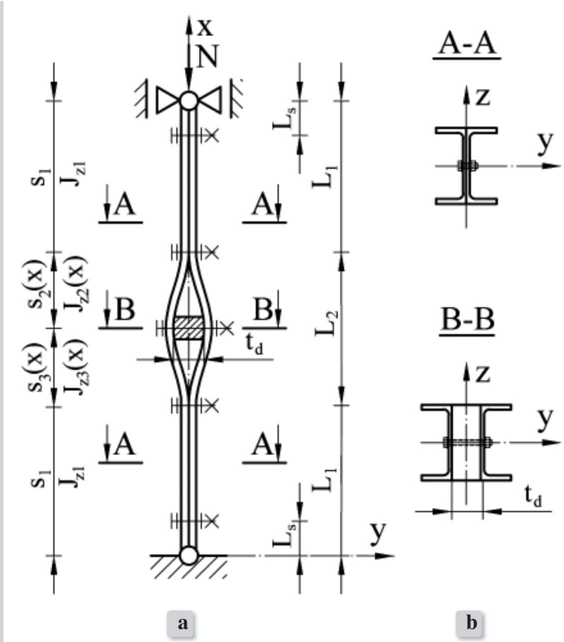

Figure 4.
Geometry of an example BPCSBUM with two-sided pinned support (a) view, (b) cross-sections

The transverse dimensions of the CSBUM chord cross-section (flange width – b_f, flange thickness – t_f, web height – h_w, web thickness – t_w) were assumed as deterministic, fixed along the member length, equal to rated dimensions.

It was assumed, in the BPCSBUM shaping, that two following parameters could be controlled: the thickness of the spacer t_d and/or the prestressing zone length L_2.

3. GEOMETRY OF BPCSBUM

The spindle shape of BPCSBUM in the prestressing zone determines its geometrical properties. Figure 4 shows an example of geometry of BPCSBUM with two-sided pinned support. Functions describing the distance $s_i(x)$ between the chords in the clear, the moment of inertia $J_i(x)$ to the main axes and the eccentricity $e_i(x)$ of the compressive force were defined for this member.

In cross-sections, where friction grip bolts are used to join chords, rigid connections were placed due to the lack of free rotation of a single chord (Fig. 5).

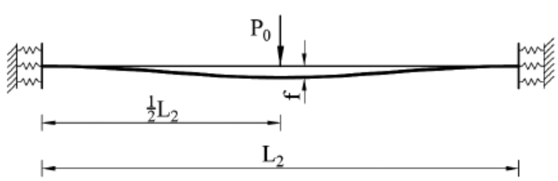

Figure 5.
Static model of the CSBUM chord in the prestressing zone

Thus, bipolar prestressing of the member was performed in the middle section of the length L_2, the initial displacement of chords $y_0(x)$ is described with cubic curves developed analogously to the deflection curve of the member anchored on two sides.

Taking into account the designations from Fig. 4 and the maximum displacement of chords in the middle of the span equal to $f = \frac{s_{max}}{2}$ the initial displacement curve $y_{0i}(x)$ was entered with two functions, respectively in the following ranges:

for $x \in \langle L_1; 0{,}5\,L \rangle$

$$y_{01}(x) = -\frac{2 \cdot s_{max}}{L_2^3}\left[4\,(x - L_1)^3 - 3\,L_2\,(x - L_1)^2\right], \quad (1)$$

and for $x \in \langle 0{,}5\,L; L - L_1 \rangle$

$$y_{02}(x) = \left\{\frac{2\,s_{max}}{L_2^3}\left[4\left(x - \frac{L}{2}\right)^3 - 3\,L_2\left(x - \frac{L}{2}\right)^2\right]\right\} + \frac{s_{max}}{2}. \quad (2)$$

The distance between the chords in the clear is variable on the member length. On the extreme sections with the length L_1 (for $x \in \langle 0; L_1 \rangle$ and $x \in \langle L-L_1; L \rangle$), the chords are joined in direct contact, therefore the distance $s_i(x)$ between the member chords is constant over the entire length and is

$$s_1 = 0. \quad (3)$$

Functions determining the distance between the chords in the clear were developed based on the curves describing the initial deflection curve (1) and (2) of the member chords in the prestressing zone:

for $x \in \langle L_1; 0{,}5\,L \rangle$

$$s_2(x) = 2\left\{-\frac{2 \cdot s_{max}}{L_2^3}\left[4\,(x - L_1)^3 - 3\,L_2\,(x - L_1)^2\right]\right\}, \quad (4)$$

for $x \in \langle 0{,}5\,L; L - L_1 \rangle$

$$s_3(x) = 2 \cdot \left\{\left\{\frac{2\,s_{max}}{L_2^3}\left[\begin{matrix}4\left(x - \frac{L}{2}\right)^3 - \\ 3\,L_2\left(x - \frac{L}{2}\right)^2\end{matrix}\right]\right\} + \frac{s_{max}}{2}\right\}. \quad (5)$$

The moments of inertia $J_i(x)$ relative to the main axes were determined as for the multiple-chord member. The factor related to the moment of inertia of the spacer was not taken into account in the middle section, arbitrarily considering its impact as negligibly low. Considering the above, the moment of inertia J_y to the material axis y is constant, described by the known relationship:

$$J_y = 2J_{y,ch}. \quad (6)$$

The moment of inertia $J_{zi}(x)$ of the cross-section with respect to the non-material axis, due to the different length of the member between the chords $s_i(x)$, was described by the function:

$$J_{zi}(x) = 2A_{ch}\left[i_{z,ch}^2 + \left(\frac{s_i(x)}{2} + e_{z,ch}\right)^2\right]. \quad (7)$$

After taking into account (3)–(5), the moments of inertia $J_{zi}(x)$ for BPCSBUM can be written for the extreme section, for $x \in \langle 0; L_1 \rangle$ and $x \in \langle L-L_1; L \rangle$, in the form of:

$$J_{z1} = 2A_{ch}\left(i_{z,ch}^2 + e_{z,ch}^2\right). \quad (8)$$

However, for the prestressing zone in the $x \in \langle L_1; 0.5L\rangle$ following ranges:

$$J_{z2}(x) = 2\,A_{ch}\left\{ i_{z,ch}^2 + \left[-\frac{2\cdot s_{\max}}{L_2^3}\begin{bmatrix} 4\,(x-L_1)^3 \\ -3\,L_2\,(x-L_1)^2 \end{bmatrix} + e_{z,ch} \right]^2 \right\} \tag{9}$$

and $x \in \langle 0.5L;\, L–L_1\rangle$:

$$J_{z3}(x) = 2\,A_{ch}\left\{ i_{z,ch}^2 + \left\{ \left[\frac{2\cdot s_{\max}}{L_2^3}\begin{pmatrix} 4\left(x-\frac{L}{2}\right)^3 - \\ 3\,L_2\left(x-\frac{L}{2}\right)^2 \end{pmatrix} \right] + \frac{s_{\max}}{2} + e_{z,ch} \right\}^2 \right\}. \tag{10}$$

In addition, to maintain the buckling direction, it is necessary to maintain the proportion of moments of inertia of the BPCSBUM:

$$\frac{J_z(x=0{,}5\,L)}{J_y} \le 1{,}0\,, \tag{11}$$

The moment of inertia of the section $J_{zi}(x)$ to the z axis is a function of the distance $s_i(x)$ between the chords in the clear. The equivalent moment of inertia $J_{z,sr}$ to the axis from the BPCSBUM cross-section is proposed as an arithmetic mean weighted from arithmetic means of moments of inertia determined on the extreme and middle sections, with a convex combination:

$$J_{z,sr} = \frac{2\cdot\frac{L_1}{L}\cdot J_{z1} + \frac{L_2}{2L}\cdot\frac{J_{z1}+J_{z2}(x=0.5\,L)}{2} + \frac{L_2}{2L}\cdot\frac{J_{z1}+J_{z3}(x=0.5\,L)}{2}}{2\cdot\frac{L_1}{L}+\frac{L_2}{2L}+\frac{L_2}{2L}}\,. \tag{12}$$

Given that:

$$J_{z2}(x=0{,}5\,L) = J_{z3}(x=0{,}5\,L), \tag{13}$$

equivalent moment of inertia $J_{z,sr}$ can be written as follows:

$$J_{z,sr} = 2\cdot\frac{L_1}{L}\cdot J_{z1} + \frac{L_2}{2L}\cdot\left(J_{z1}+J_{z2}(x=0{,}5\,L)\right). \tag{14}$$

The eccentricity e_{zi} of the compressive force N on the BPCSBUM chords is represented by the following formula:

$$e_{zi}(x) = e_{z,ch} + \frac{s_i(x)}{2}. \tag{15}$$

For the extreme sections – for $x \in \langle 0;L_1\rangle$, $x \in \langle L–L_1;L\rangle$ – it is equal to the distance describing the centre of gravity position of the single chord section:

$$e_{z1} = e_{z,ch}\,. \tag{16}$$

In the prestressing zone, the eccentricity $e_{zi}(x)$ of the compressive force N on the BPCSBUM chords is described by the functions:

for $x \in \langle L_1; 0.5L\rangle$

$$e_{z2}(x) = e_{z,ch} + \frac{s_2(x)}{2}, \tag{17}$$

for $x \in \langle 0.5L;\, L–L_1\rangle$

$$e_{z3}(x) = e_{z,ch} + \frac{s_3(x)}{2}. \tag{18}$$

4. ASSESSMENT OF CAPACITY – ANALYTICAL ESTIMATION

At the end of the 19th century, Engesser [12,13,16] was the first to consider shear stiffness when analysing the built-up compressed member. He estimated the critical load bearing capacity N_{cr}^{Eng} using a linear interaction of local and global critical load bearing capacity. A fairly simple formula (19) associated with Euler critical load capacity N_e is known in the form of:

$$N_{cr}^{Eng} = \frac{N_e}{1+N_e/S_v}\,. \tag{19}$$

To estimate the critical load capacity of the BPCSBUM, a modification of the Engesser's formula (19) was proposed allowing for a far-reaching simplification of the problem at the expense of a small loss of estimation accuracy. Introduction of the critical force N_{eb} of the BPCSBUM described by the following formula (20) is suggested in place of the Euler critical load capacity N_e:

$$N_{eb} = \frac{\pi^2\,E\,J_{z,sr}}{L^2}\,. \tag{20}$$

The shear stiffness S_v is proposed to be estimated on the basis of the relationship (21) derived for a two-chord member with rigid battens [14]

$$S_v = \frac{24\,E\,J_{z,ch}}{L_b^2}\,, \tag{21}$$

where:

$$L_b = L_1 - L_s\,. \tag{22}$$

The modified Engesser's formula (19) will therefore take the form:

$$N_{cr}^{\mathrm{mod}} = \frac{N_{eb}}{1 + N_{eb}/S_v}\,. \tag{23}$$

5. FINITE ELEMENT ANALYSIS (FEA) OF BPCSBUM

The issue of stability of the BPCSBUM was solved by the FEM using the commercial ABAQUS/CAE software[43–45]. The steel asymmetrical members made of a pair of channel sections were subjected to simulation.

5.1. Finite Element Type and Mesh

A spatial and shell model was made. The S4R Shell Finite Element, available in the software library, was applied. It is an element with linear shape functions and reduced numerical integration. Simulations for the standard and BPCSBUM were performed with the assumption of the finished element dimension not greater than 10×10 [mm]. An example of finite element grid was shown in Fig. 6.

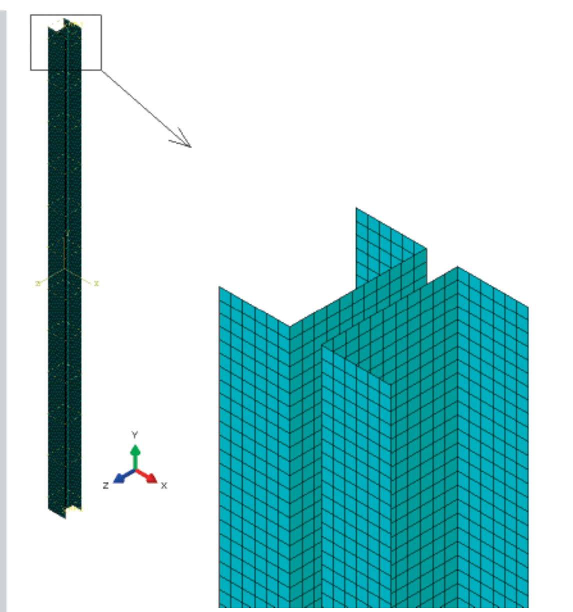

Figure 6.
An example of finite element grid

5.2. Material Model

A model of an ideally elastic-plastic isotropic material was adopted. The material was defined by the Young's modulus, Poisson's ratio and density. The standard values specified for steel in [41] were assumed, and thus: Young's modulus E = 210 GPa, Poisson's ratio $\nu = 0.3$ and density $\rho = 7800$ kg/m^3.

5.3. Contact

The contact was defined between chords and a spacer and between each of the chords.

The contact between chords and a spacer was defined in the form of general contact with properties of normal behavior as "hard" contact with the possibility of separation after contact. General contact interactions allow to define contact between many regions of the model with a single interaction. The general contact algorithm uses the finite-sliding, surface-to-surface contact formulation and a penalty method to enforce active contact constraints.

The contact between chords was defined in the form of surface-to-surface contact with properties of normal behavior as "hard" contact and tangential behavior using penalty method with friction coefficient 0.1.

The bolt in the middle of the member span joining the chords with the spacer was modelled as a beam-type connector with a diameter corresponding to the diameter of the bolt.

5.4. Steps

Analysis of the BPCSBUM was divided into three calculation steps:

- Initial,
- Prestressing,
- Buckle.

In the *Initial* step, the contact between the spacer and chords of the CSBUM was defined.

The calculation step *Prestressing* was created to obtain a non-linear geometry of a CSBUM. On the perimeter of the spacer the possibility of translational displacements was blocked in all directions. The displacement of connections corresponding to the locations of the friction grip bolts in the direction z was defined (U3 = $0.5s_{max}$= $0.5t_d$).

Calculation step *Buckle* was created to analyze the stability of the BPCSBUM. Reference points were created in which the pinned support of the member was modelled in the axis of the member, 10 mm above and below its contour. Then continuum distributing couplings were created with which all edge degrees of freedom were associated with the corresponding reference point. A compressive load in the form of an axial force with a nominal value of 1 N was defined. Linear buckling analysis (LBA) was performed. The result of the simulation is the multiplier of the critical load and the buckling form of the BPCSBUM.

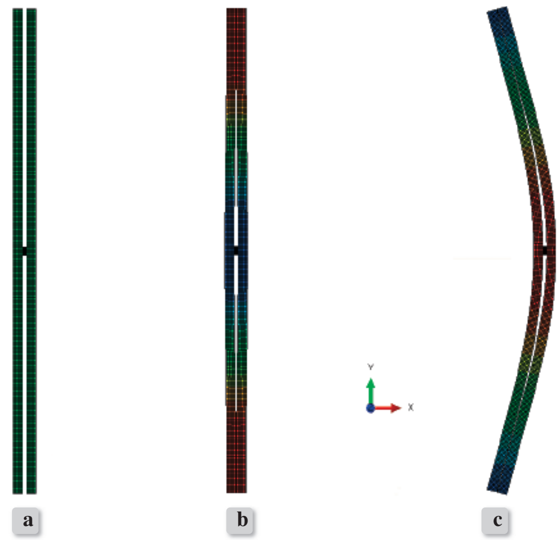

Figure 7.
An example of a BPCSBUM – calculation steps: (a) Initial, (b) Prestressing, (c) Buckling analysis

6. RESULTS

The study covered the standard CSBUM made of the rolled channel sections UPE120 and UPE160 (Tab. 1) joined in direct contact in four places with M16 bolts spaced at $L_b = 950$ mm (Fig. 8a) and BPCSBUM made of the same sections (Fig. 8b).

A length was assumed for all members $L = 3.0$ m. The prestressing range L_2 was analysed in two variants: $0.7L = 2100$ mm and $0.8L = 2400$ mm. Thickness of the spacer $t_d = s_{max}$ was changed in the range from 4–12 mm in increments of 4 mm. The width of the spacer was assumed $b = 50$ mm.

Table 1.
Geometric characteristics of UPE120 and UPE160

Section	A_{ch}	$J_{y,ch}$	$J_{z,ch}$	$i_{z,ch}$	$e_{z,ch}$
	[cm^2]	[cm^4]	[cm^4]	[cm]	[cm]
UPE120	16.8	392	60.7	1.90	2.02
UPE160	23.7	965	114	2.19	2.20

The critical load capacity of the standard closely spaced built-up member, estimated with the Engesser's formula, (19) respectively for:

- UPE 120: $N_{cr}^{Eng} = 506.4$ kN;
- UPE 160: $N_{cr}^{Eng} = 903.8$ kN.

Table 2 presents the description of the geometries considered in the BPCSBUM example, developed on the basis of the formulas presented in section 3.

Figures 9 and 10 show the result of FEM simulation for BPCSBUM with the geometry analyzed in the example. All of the tested members lost their stability assuming the first form of buckling in the form of a sinusoidal half-wave.

Critical load capacity of BPCSBUM estimated by modified Engesser's (28) and FEM formula is presented in Table 3. In addition, there are also:

- analytically obtained percentage comparison of the critical load capacities of BPCSBUM (N_{cr}^{S}) with formula (23) and FEM ($N_{cr,\,PBSB}^{MES}$) by relationship:

$$\zeta_1 = \frac{N_{cr}^{S} - N_{cr,PBSB}^{MES}}{N_{cr,PBSB}^{MES}} \cdot 100\% . \tag{24}$$

Table 2.
Description of the BPCSBUM geometry

2xUPE120									
L_2	[mm]	2100				2400			
t_d	[mm]	4	8	12	16	4	8	12	16
J_{z1} (8)	[cm^4]	258.50							
$J_{z2}(x=150.0)$ (9)	[cm^4]	286.99	318.18	352.04	388.60	286.99	318.18	352.04	388.60
$J_{z,sr}$ (14)	[cm^4]	268.48	279.39	291.24	304.04	269.90	282.37	295.92	310.54
2xUPE160									
L_2	[mm]	2100				2400			
t_d	[mm]	4	8	12	16	4	8	12	16
J_{z1} (8)	[cm^4]	457.42							
$J_{z2}(x=150.0)$ (9)	[cm^4]	501.02	548.42	599.62	654.60	501.02	548.42	599.62	654.60
$J_{z,sr}$ (14)	[cm^4]	472.68	489.27	507.19	526.43	474.86	493.82	514.30	536.29

- increased critical load capacity of BPCSBUM (N_{cr}^{mod}) in comparison to the critical load capacity of the standard CSBUM (N_{cr}^{Eng}) estimated analytically by formulas (23) and (19) according to the following relationship:

$$\zeta_2 = \frac{N_{cr}^{\mathrm{mod}} - N_{cr}^{Eng}}{N_{cr}^{Eng}} \cdot 100\% . \qquad (25)$$

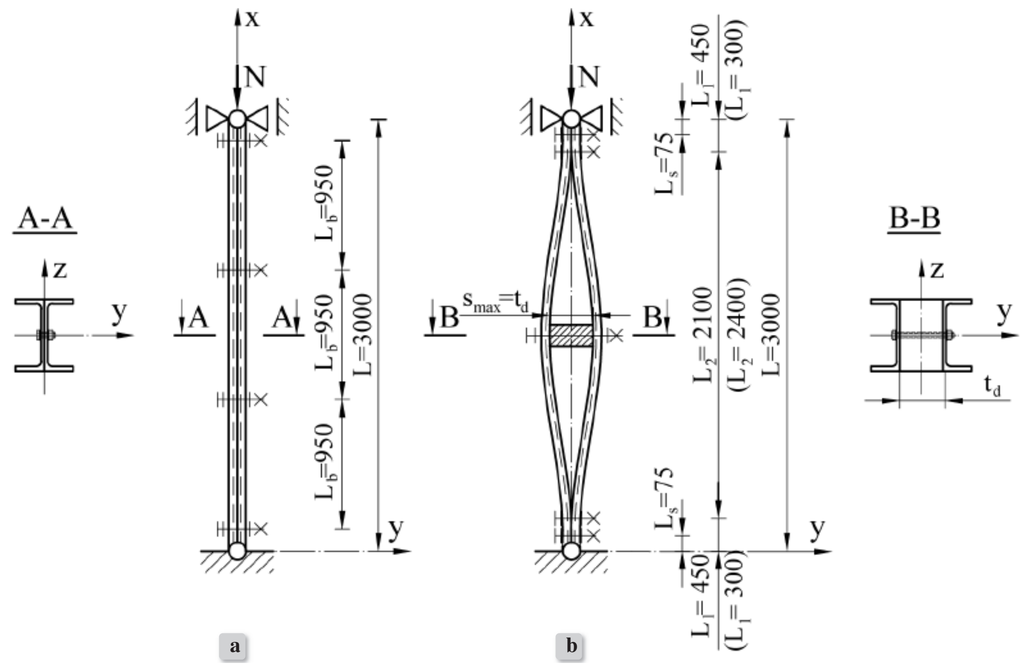

Figure 8.
Calculation example (a) standard CSBUM (b) BPCSBUM

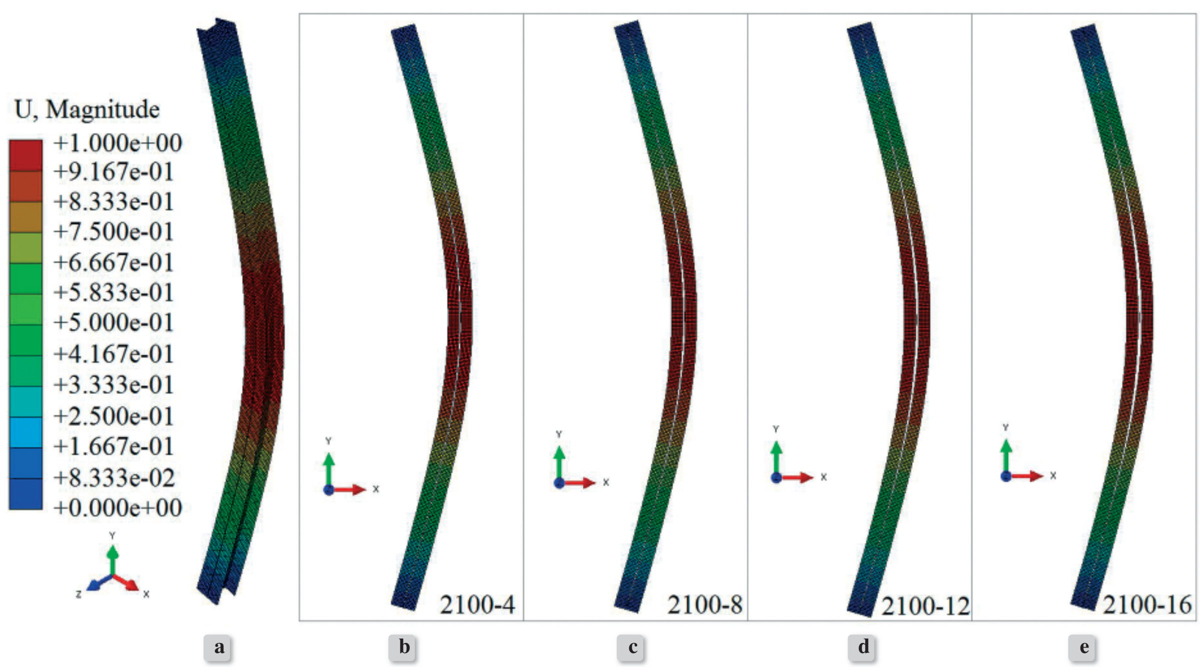

Figure 9.
The result of FEM simulation on BPCSBUM built from a pair of UPE120 channel sections with the length of the prestressing zone L_2 = 2100 mm: (a) 3D view, (b)–(e) 2D view according to the thickness of the spacer t_d: (b) t_d = 4 mm, (c) t_d = 8 mm, (d) t_d = 12 mm, (e) t_d = 16 mm

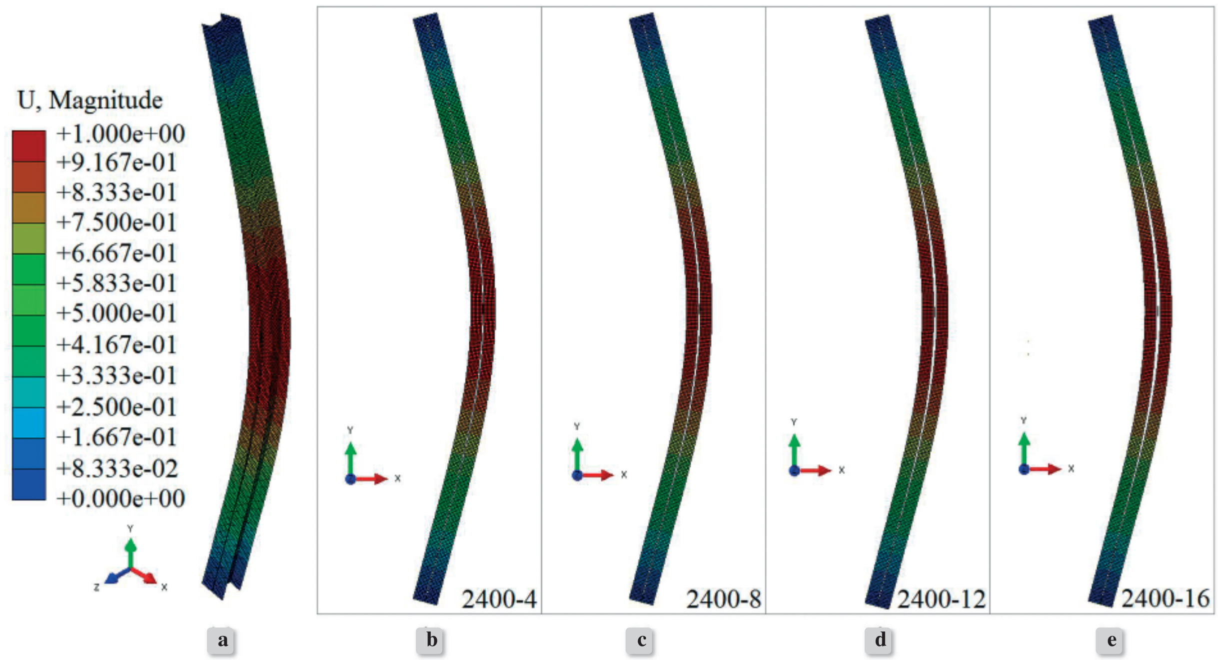

Figure 10.
The result of FEM simulation on BPCSBUM built from a pair of UPE120 channel sections with the length of the prestressing zone L_2 = 2100 mm: (a) 3D view, (b)–(e) 2D view according to the thickness of the spacer t_d: (b) t_d = 4 mm, (c) t_d = 8 mm, (d) t_d = 12 mm, (e) t_d = 16 mm

Table 3.
Critical load capacity of BPCSBUM

L_2	$t_d=s_{max}$	N_{cr}^{mod} (23)	$N_{cr,PBSB}^{MES}$	ζ_1	ζ_2
[mm]	[mm]	[kN]	[kN]	[%]	[%]
2xUPE120					
2100	4	601.2	594.4	1.14	18.72
	8	624.9	631.8	-1.09	23.40
	12	650.6	671.1	-3.06	28.48
	16	678.3	712.0	-4.73	33.95
2400	4	615.2	570.9	7.76	21.49
	8	643.4	608.1	5.81	27.05
	12	673.9	647.7	4.05	33.08
	16	706.8	689.5	2.51	39.57
2xUPE160					
2100	4	1060.3	1043.0	1.66	17.32
	8	1096.5	1097.0	-0.05	21.32
	12	1135.5	1154.2	-1.62	25.64
	16	1177.3	1180.2	-0.25	30.26
2400	4	1083.1	1005.8	7.69	19.84
	8	1125.9	1061.0	6.12	24.57
	12	1172.1	1119.1	4.74	29.69
	16	1221.7	1187.8	2.85	35.17

Differences between the obtained analytically critical load bearing capacity of BPCSBUM and FEM were within the following ranges:

- -4.73% ÷ 7.76% for 2x UPE 120;
- -1.62% ÷ 7.69% for 2x UPE160.

The results for the BPCSBUM analyzed in the exam-

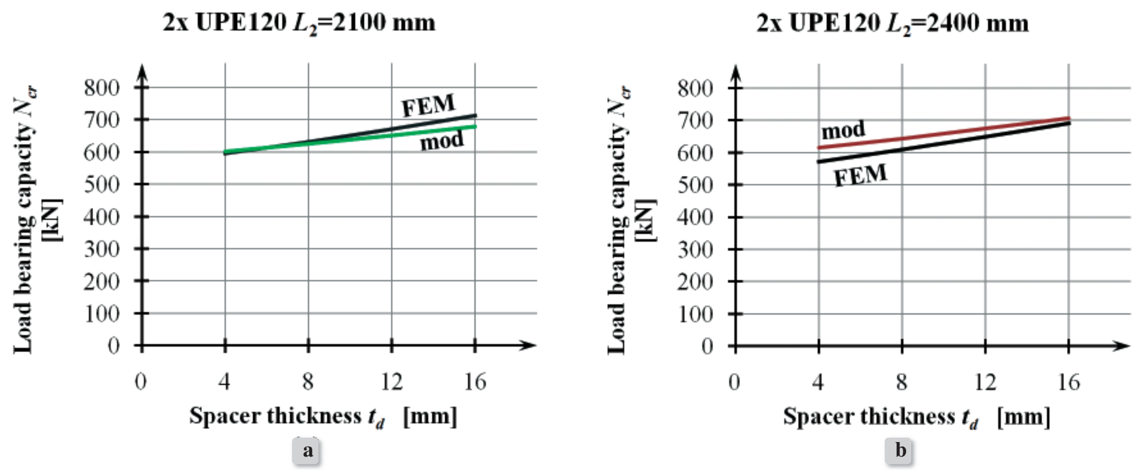

Figure 11.
Comparison of numerical (FEM) and analytical (mod) results for BPCSBUM: (a) 2xUPE120, L_2 = 2100 mm, (b) 2xUPE120, L_2 = 2400 mm

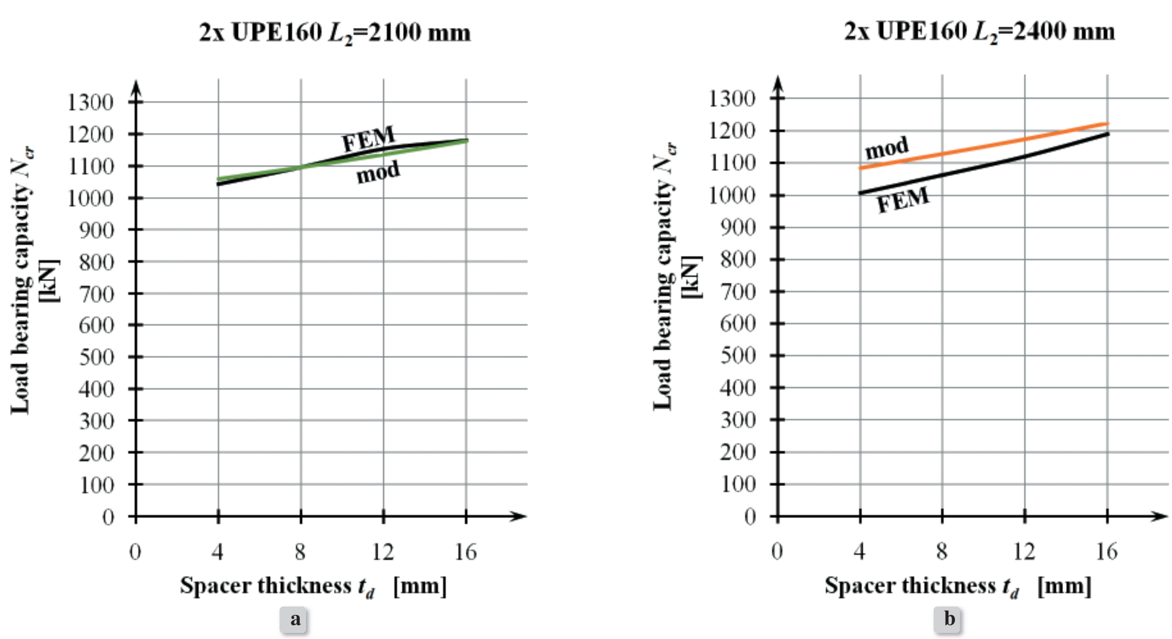

Figure 12.
Comparison of numerical (FEM) and analytical (mod) results for BPCSBUM: (a) 2xUPE160, L_2 = 2100 mm, (b) 2xUPE160, L_2 = 2100 mm

ple are shown in Figures 11 and 12. Good agreement between the results obtained with the modified Engesser's (28) and FEM formula was shown.

Figure 13 was made based on the analytical results and shows the critical load bearing capacity gain of the BPCSBUM compared to the load bearing capacity of the standard back-to-back CSBUM joined with 4 bolts. The axes of the graph are described as follows:

- horizontal axis – thickness of spacer t_d;
- vertical axis – a dimensionless coefficient, i.e. the proportion of the critical load bearing capacity of BPCSBUM N_{cr}^{mod} to the critical load bearing capacity of a standard CSBUM joined with 4 bolts N_{cr}^{Eng}.

Graphs for the prestressing zone length were drawn up $L_2 = 0.7L = 2100$ mm and $L_2 = 0.8L = 2400$ mm.

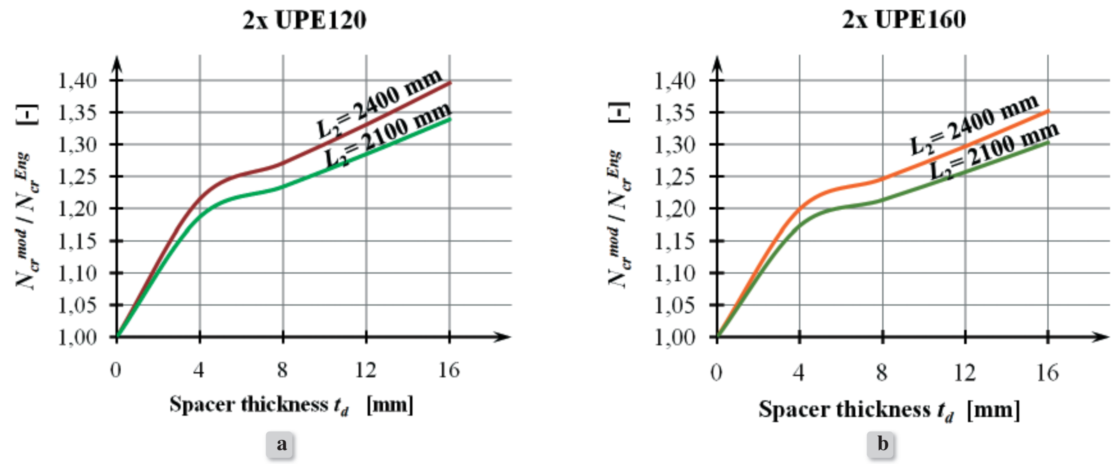

Figure 13.
Critical load bearing capacity of BPCSBUM built of: (a) 2xUPE120, (b) 2xUPE160

7. SUMMARY AND CONCLUSIONS

(1) The studies presented in this paper relate to the BPCSBUM. The literature on CSBUMs is extensive, but there are no studies on BPCSBUM for which a correct description of geometry is indispensable to start static and strength analyzes.

(2) A high convergence of critical load bearing capacity of BPCSBUM estimated from the modified Engesser's (23) and FEM formula was obtained. For considered prestressing zone length $L_2 = 0.7L$ in the BPCSBUM example, the differences are up to 3%, while for the prestressing range $L_2 = 0.8L$ do not exceed 8%.

(3) In connection with the possibility of applying bipolar prestressing by displacement to reinforce the structure of CSBUMs:

- an equivalent moment of inertia $J_{z,sr}$ can be applied to pre-estimate the critical load bearing capacity of BPCSBUM with the formula (23);
- using the relationship (25), it is possible to predict an increase in the load bearing capacity of the CSBUM under bipolar prestressing.

(4) For the BPCSBUM considered in the example, the predicted load bearing capacity gain with a 4 mm spacer is nearly 20%. However, when using a 16 mm spacer, it is 30–40%. Therefore it is possible to **increase the critical bearing load capacity** of a CSBUM by bipolar prestressing above the critical load bearing capacity of a standard CSBUM.

Further analytical, numerical and experimental tests are planned for the load bearing capacity and stability of the BPCSBUM, in particular with other chord sections, different spacer thickness and the prestressing zone lengths.

REFERENCES

[1] Chesson, E. Jr., & Munse, W. H. (1963). Riveted and Bolted Joints: Truss-Type Tensile Connections. *J. Struct. Div., 89*(1), 67–106.

[2] McCormac, M. C., & Csernak, S. F. (2012). Structural steel design. New Jersey: Prentice Hall.

[3] Subramanian, N. (2010). Steel Structures. Design and practice. New Delhi: Oxford University Press.

[4] Büttner, O., & Stenker, H. (1975). Light metal constructions. Warsaw: Arkady. (in Polish)

[5] Space structures (1985). edited by Bródka, J. Arkady: Warsaw. (in Polish)

[6] Chilton, J. (2000). Space grid structures. Oxford: Architectural Press.

[7] Porto, C. E. (2014). The innovative structural conception in Stéphane du Château's work: from metallic trusses to the development of spatial frames. *Architectus* 4, 51–64.

[8] Kowal, Z. (2011). The formation of space bar structures supported by the system reliability theory. *Arch. Civ. Mech. Eng. 11*(1), 115–133.

[9] Kowal, Z., Piotrowski, R., & Szychowski, A. (2012). Adaptation of halls with roof covering to solar radiation energy extraction. *Zeszyty Naukowe Politechniki Rzeszowskiej,* 283, *59*(2/2012/II), 431–438 (in Polish).

[10] Kowal, Z., Siedlecka, M., Piotrowski, R., Brzezińska, K., Otwinowska, K., & Szychowski, A. (2015). Shapes of energy-active segments of steel buildings. *Arch. Civ. Eng., 61*(3), 119–132.

[11] Kubicka, K., Radoń, U., Szaniec, W., & Pawlak, U. (2017). Comparative Analysis of the Reliability of Steel Structure with Pinned and Rigid Nodes Subjected to Fire. *IOP Conf. Ser.: Mater. Sci. Eng*. 245, 022051 1–9.

[12] Timoshenko, S. P. (1966). History of strength of materials. Warsaw: Arkady (in Polish).

[13] Engesser, F. (1889). Über Knickfestigkeitgerader Stäbe. Zeitschriftfür *Architekten und Ingenieurwesen, 35*(4), 455–462.

[14] Haringx, J. A. (1949). Elastic stability of helical springs at a compression larger than original length. *Appl. Sci. Res., 1*(1), 417–434.

[15] Bleich, F. (1952). Buckling strength of metal structures. New York: Mc Graw-Hill.

[16] Timoshenko, S. P., & Gere, J. M. (1963). Theory of elastic stability. Warsaw: Arkady (in Polish).

[17] Kowal, Z. (2001). About the critical load bearing capacity of battened columns. *Inżynieria i Budownictwo*, 10, 580–582 (in Polish).

[18] Bažant, Z. P. (2003). Shear Buckling of Sandwich, Fiber Composite and Lattice Columns, Bearings, and Helical Springs: Paradox Resolved. *J. Appl. Mech*., 70, 75–83.

[19] Aslani, F., & Goel, S. C. (1991). An Analytical Criterion for Buckling Strength of Built-up Compression Members. *Eng. J., 28*(4), 159–168.

[20] AISC LRFD: 1994. Load and resistance factor design, American Institute of Steel Construction (AISC), Chicago.

[21] Temple, M. C., & El-Mahdy, G. M. (1993). Buckling of built-up compression members in the plane of the connectors. *Can. J. Civ. Eng.,* 20, 895–909.

[22] Temple, M. C., & El-Mahdy, G. M. (1995). Local effective length factor in the equivalent slenderness ratio. *Can. J. Civ. Eng*., 22, 1164–1170.

[23] Lue, D. M., Yen, T., & Liu, J. L. (2006). Experimental Investigation on Built-up Columns. *J. Constr. Steel Res*., 62, 1325–1332.

[24] Liu, J. L., Lue, D. M., & Lin, Ch. H. (2009). Investigation on Slenderness Ratios of Built-up Compression Members. *J. Constr. Steel Res*., 65, 237–248.

[25] AISC-LRFD:2005. Load and resistance factor design. Specification for structural steel buildings. American Institute of Steel Construction: Chicago.

[26] AS-4100:1998. Steel structures. Standards Association of Australia, Homebush, Australia, 1998.

[27] CSA S16-01:2001. Limit states design of steel structures. Canadian Standards Association, Toronto.

[28] Abejide, O. S., & Masce, P. E. (2007). Evaluation of Effective Lengths of Braced Double Angle Diagonals. *Res. J. Appl. Sci, 2*(10), 1060–1065.

[29] CEN: 2003. Eurocode 3: Design of Steel Structures. Part 1-1: General Rules and Rules for Buildings. European Committee for Standardization.

[30] AISC: 1999. Load and resistance factor design. Specification for structural steel buildings. American Institute of Steel Construction, Chicago.

[31] BS5950: 2000. Structural Use of Steelwork in Buildings. British Standards Institution, London.

[32] Stone, T. A., & La Boube, R. A. (2005). Behavior of cold-formed steel built-up I-sections. *Thin-Walled Struct*., 43, 1805–1817.

[33] Ting, T. C. H., & Lau, H. H. (2011) Compression Test on Cold-formed Steel Built-up Back-to-back Channels Stub Columns. *Adv. Mater. Res*., 201–203: 2900–2903.

[34] Anbarasu, M., Kanagarasu, K., & Sukumar, S. (2015). Investigation on the behaviour and strength of cold-formed steel web stiffened built-up battened columns. *Mater. and Struct.*, 48, 4029–4038.

[35] Zhang, J.-H., & Young, B. (2015). Numerical investigation and design of cold-formed steel built-up open section columns with longitudinal stiffeners. *Thin-Walled Struct*., 89, 178–191.

[36] Tamai, H., Yamanishi, T., Takamatsu, T. & Matsuo, A. (2011). Experimental study on lateral buckling behavior of weld-free built-up member made of H-SA700A high-strength steel. *J. Struct. Constr. Eng*. 2, 407–415.

[37] Słowiński, K., & Wuwer, W. (2016). Blind-bolted shear connections for axially compressed RHS columns strengthened with open sections. *J. Constr. Steel Res*. 127, 15–27.

[38] Słowiński, K., & Wuwer, W. (2016). Technology of reinforcing of compressed steel bars with closed and open cross-sections. *Fastener: rynek elementów złącznych*, 1, 43–47.

[39] Deniziak, P., & Winkelmann, K. (2018). TS-based RSM-aided design of cold-formed steel stiffened C-sectional columns susceptible to buckling, *Shell Struct.: Theory and Applications*, 4, 533–536.

[40] Deniziak, P., & Winkelmann, K. (2018). Influence of nonlinearities on the efficiency and accuracy of FEM calculations on the example of a steel build-up thin-walled column. *MATEC Web of Conferences*, 219, 02010 1–8.

[41] PN-EN 1993-1-1:2006 Eurocode 3: Design of steel structures – Part 1-1: General rules and rules for buildings. The Polish Committee for Standardization, Warsaw.

[42] Kowal, Z., & Siedlecka, M. (2017). Load bearing capacity of compressed closely spaced built-up members in space structures. *JCEEA*, *34, 64*(3/I/17), 407–416.

[43] ABAQUS 6.14. PDF Documentation. Abaqus Analysis User's Guide, Simulia, Dassault Systèmes, 2014.

[44] ABAQUS 6.14. PDF Documentation. Abaqus/CAE User's Guide, Simulia, Dassault Systèmes, 2014.

[45] ABAQUS 6.14. PDF Documentation. Abaqus Theory Guide, Simulia, Dassault Systèmes 2014.